

# Regenerative Capacity of Alveolar Type 2 Cells Is Proportionally Reduced Following Disease Progression in Idiopathic Pulmonary Fibrosis-Derived Organoid Cultures

<https://doi.org/10.4046/trd.2024.0094>

ISSN: 1738-3536(Print/)

2005-6184(Online)

Tuberc Respir Dis 2025;88:130-137



Copyright © 2025 The Korean Academy of Tuberculosis and Respiratory Diseases

**Address for correspondence****Moo Suk Park, M.D., Ph.D.**

Division of Pulmonary and Critical Care Medicine, Department of Internal Medicine, Severance Hospital, Yonsei University College of Medicine, 50-1 Yonsei-ro, Seodaemun-gu, Seoul 03722, Republic of Korea

Phone 82-2-2228-1955

E-mail pms70@yuhs.ac

Received Jul. 4, 2024

Revised Sep. 14, 2024

Accepted Sep. 22, 2024

Published online Sep. 27, 2024

Hyeon Kyu Choi, M.D.<sup>1</sup>, Gaeul Bang, M.S.<sup>2</sup>, Ju Hye Shin, M.S.<sup>3</sup>, Mi Hwa Shin, B.S.<sup>3</sup>, Ala Woo, M.D.<sup>3</sup>, Song Yee Kim, M.D., Ph.D.<sup>3</sup>, Sang Hoon Lee, M.D., Ph.D.<sup>3</sup>, Eun Young Kim, M.D., Ph.D.<sup>3</sup>, Hyo Sup Shim, M.D., Ph.D.<sup>4</sup>, Young Joo Suh, M.D., Ph.D.<sup>5</sup>, Ha Eun Kim, M.D.<sup>6</sup>, Jin Gu Lee, M.D., Ph.D.<sup>6</sup>, Jinwook Choi, Ph.D.<sup>2,7</sup>, Ju Hyeon Lee, Ph.D.<sup>7</sup>, Chul Hoon Kim, M.D., Ph.D.<sup>1</sup> and Moo Suk Park, M.D., Ph.D.<sup>3</sup>

<sup>1</sup>Department of Pharmacology, Yonsei University College of Medicine, Seoul, <sup>2</sup>School of Life Sciences, Gwangju Institute of Science and Technology, Gwangju, <sup>3</sup>Division of Pulmonary and Critical Care Medicine, Department of Internal Medicine, Severance Hospital, Yonsei University College of Medicine, Seoul, Departments of <sup>4</sup>Pathology, <sup>5</sup>Radiology, Yonsei University College of Medicine, Seoul, <sup>6</sup>Department of Thoracic and Cardiovascular Surgery, Severance Hospital, Yonsei University College of Medicine, Seoul, Republic of Korea, <sup>7</sup>Welcome-MRC Cambridge Stem Cell Institute, Jeffrey Cheah Biomedical Centre, University of Cambridge, Cambridge, United Kingdom

**Abstract**

**Background:** Idiopathic pulmonary fibrosis (IPF) is a chronic, progressive lung disease that culminates in respiratory failure and death due to irreversible scarring of the distal lung. While initially considered a chronic inflammatory disorder, the aberrant function of the alveolar epithelium is now acknowledged as playing a central role in the pathophysiology of IPF. This study aimed to investigate the regenerative capacity of alveolar type 2 (AT2) cells using IPF-derived alveolar organoids and to examine the effects of disease progression on this capacity.

**Methods:** Lung tissues from three pneumothorax patients and six IPF patients (early and advanced stages) were obtained through video-assisted thoracoscopic surgery and lung transplantation. HTII-280+ cells were isolated from CD31-CD45-epithelial cell adhesion molecule (EpCAM)+ cells in the distal lungs of IPF and pneumothorax patients using fluorescence-activated cell sorting (FACS) and resuspended in 48-well plates to establish IPF-derived alveolar organoids. Immunostaining was used to verify the presence of AT2 cells.

**Results:** FACS sorting yielded approximately 1% of AT2 cells in early IPF tissue, and the number decreased as the disease progressed, in contrast to 2.7% in pneumothorax. Additionally, the cultured organoids in the IPF groups were smaller and less numerous compared to those from pneumothorax patients. The colony forming efficiency decreased as the disease advanced. Immunostaining results showed that the IPF organoids expressed less surfactant protein C (SFTPC) compared to the pneumothorax group and contained keratin 5+ (KRT5+) cells.

**Conclusion:** This study confirmed that the regenerative capacity of AT2 cells in IPF decreases as the disease progresses, with IPF-derived AT2 cells inherently exhibiting functional abnormalities and altered differentiation plasticity.

**Keywords:** Idiopathic Pulmonary Fibrosis; Alveolar Type 2 Cells; Patient-Derived Lung Organoid; Lung Regeneration



© It is identical to the Creative Commons Attribution Non-Commercial License (<http://creativecommons.org/licenses/by-nc/4.0/>).

## Introduction

Idiopathic pulmonary fibrosis (IPF) is a chronic, progressive lung disease that leads to respiratory failure and death due to irreversible scarring of the distal lung<sup>1-3</sup>. Traditionally, it was believed that excessive immune system inflammation caused IPF lung fibrosis, but large-scale clinical studies using immunosuppressants have shown these treatments increase mortality and accelerate disease progression in pulmonary fibrosis patients<sup>4</sup>. Current understanding suggests that IPF pathogenesis may involve the deregulation of alveoli regeneration<sup>5</sup>. Studies have reported shortened telomere lengths in cells from IPF patients<sup>6,7</sup>. Furthermore, in a mouse model, disrupting telomere function in alveolar stem cells proved to lead to lung fibrosis progression<sup>8,9</sup>. Recent advances in single-cell transcriptome analysis have identified a unique aberrant basaloid cell in the alveolar epithelial cells of IPF patients<sup>10,11</sup>. These cells exhibit features of epithelial-mesenchymal transition and senescence<sup>12</sup>. Additionally, a study has confirmed that human alveolar type 2 (AT2) epithelium can transdifferentiate into metaplastic keratin 5+ (KRT5+) basal cells<sup>13</sup> when co-cultured with fibroblasts from IPF patients, though it remains unconfirmed if AT2 cells from IPF patients can transdifferentiate independently. This study aims to create lung organoids at various stages of IPF to assess the regenerative capacity of AT2 cells and determine whether they can differentiate into KRT5+ basal cells autonomously.

## Materials and Methods

### 1. Subjects and tissue collection

Lung tissue samples were obtained from Severance Hospital, Yonsei University College of Medicine. Three control lung tissue samples were sourced from patients experiencing pneumothorax. Surrounding tissues were collected during the bullectomy procedure performed using video-assisted thoracoscopic surgery (VATS). The IPF patient group was categorized into two stages. Patients diagnosed initially with normal pulmonary function tests, or forced vital capacity (FVC) or diffusing capacity of the lung for carbon monoxide (DLco) of 70% or higher, and with less than 10% fibrosis on imaging were classified as early-stage IPF. Conversely, patients who had undergone lung transplantation, presenting with FVC or DLco below 40% on pulmonary function tests and more than 70% fibrosis on imaging, were classified as advanced-stage IPF. Early-stage IPF lung tissue samples were obtained via VATS biopsy (n=3). Advanced-stage IPF samples were secured from tissues post-lung transplantation (n=3) (Table 1 and Figure 1). The baseline characteristics of the three groups are detailed in (Table 1). All studies received approval from the Institutional Review Board of Severance Hospital, Yonsei University College of Medicine, Seoul (IRB no.4-2019-0447, IRB no. 4-2012-0685, and IRB no. 4-2013-0770). Written informed consent was obtained from all patients.

### 2. Lung digestion

The lung tissue samples were finely chopped using tissue scissors, then subjected to chemical dissociation

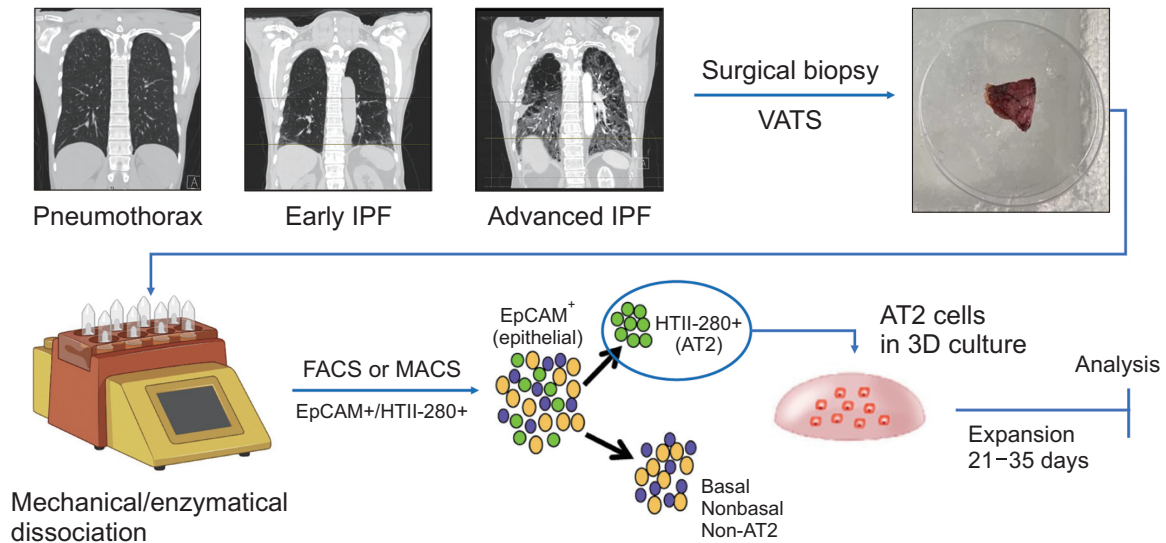
**Table 1.** Baseline characteristics of study

Characteristic	Pneumothorax (n=3)	Early IPF (n=3)	Advanced IPF (n=3)
Age, yr	19 (14–20)	61 (55–69)	61 (54–62)
Male sex	3 (100)	3 (100)	3 (100)
Smoking status			
Never smoker	3 (100)	0	0
Current smoker	0	2 (66.7)	0
Ex-smoker	0	1 (33.3)	3 (100)
Pulmonary lung function			
FVC	103.25±11.67	84.33±11.85	50±11.79
DLco	94±1.41	70.33±17.39	31.33±17.62

Values are presented as median (range), number (%), or mean±standard deviation.

IPF: idiopathic pulmonary fibrosis; FVC: forced vital capacity; DLco: diffusing capacity of the lung for carbon monoxide.

**Figure 1.** Overall experimental workflow. IPF: idiopathic pulmonary fibrosis; VATS: video-assisted thoracoscopic surgery; FACS: fluorescence activated cell sorter; MACS: magnetic associated cell separation; EpCAM: epithelial cell adhesion molecule; AT2: alveolar type 2; 3D: three-dimensional.



for approximately 40 minutes using a Gentle magnetic activated cell sorting (MACS) Octo Dissociator with Heaters (cat. no. 130-096-427; Miltenyi Biotec, Bergisch Gladbach, Germany) equipped with multi-tissue dissociation kits (cat no. 130-110-201). The dissociated cells were filtered through a 70- $\mu$ m strainer, washed, and subsequently, red blood cells lysis was carried out at room temperature for 5 minutes.

### 3. Fluorescence-activated cell sorting

The dissociated cells were resuspended in BD stain buffer (cat. no. 554656; BD Pharmingen, Becton, Dickinson and Company, Franklin Lakes, NJ, USA), transferred to individual Eppendorf (EP) tubes, and mixed with the 1st antibodies: CD31-allophycocyanin (cat no. 303116), CD45-fluorescein isothiocyanate (cat no. 304006), CD325 (epithelial cell adhesion molecule [EpCAM])-PE-cy7 (cat no. 25-9326-42), and HTII-280 (cat no. TB-27AHT2-280). The mixture was incubated on ice with occasional shaking for 30 minutes. After a washing step, the 2nd antibody BV421 (cat no. 562595) was added to the tube containing HTII-280 and incubated on ice with shaking for 20 minutes. Post-washing, the cells were transferred to a fluorescence-activated cell sorting (FACS) tube and sorted using the BD FACS Aria III machine to isolate CD31- CD45- CD325+ HTII-280+ cells.

### 4. Magnetic associated cell separation

The dissociated cells were resuspended in BD stain buffer (cat no. 554656) and incubated with CD326 magnetic beads (cat no. 130-061-101) on ice for 20 minutes. The mixture was then added to a MACS column to filter out CD326+ cells. Subsequently, HTII-280 was added, and the mixture was incubated again on ice for another 20 minutes. Following this, immunoglobulin M (IgM) beads (cat no. 130-047-302) were introduced and incubated on ice for 20 minutes. The cells were then placed into a MACS column to filter out HTII-280+ cells, and a cell count was performed.

### 5. Organoid culture and assay

AT2 cells were cultured (20,000 AT2 cells per well) in alveolar media on growth factor-reduced Matrigel (cat. no. CLS356231; Corning Inc., Corning, NY, USA). Alveolar media, comprising advanced Dulbecco's Modified Essential Medium/F-12 supplemented with SB431542, BIRB796, CHIR99021, insulin-transferrin-selenium, 4-(2-hydroxyethyl)-1-piperazineethanesulfonic acid, glutamax, heparin, B27 supplement, N-acetyl cysteine, human epidermal growth factor, hNoggin, fibroblast growth factor 7 (FGF7), FGF10, pen/strep, and primocin, was used. The cell suspension in Matrigel was placed into 48-well plates, treated with Rho-associated, coiled-coil-containing protein kinase inhibitor for the first 48 hours and with hepatocyte growth factor for 7 days. Organoids were cultured for 21 to 35 days. On

day 21, the number of organoids per well was counted to calculate colony forming efficiency (CFE) as the number of organoids per 20,000 cells. Additionally, on day 35, the organoids were cryo-sectioned to prepare for immunostaining.

### 6. Frozen section preparation

To disrupt the Matrigel dome containing the organoids, incubate in ice-cold recovery solution (cat no. 354253) at 4°C for 1 hour in an EP tube. After removing the supernatant, add 4% paraformaldehyde and incubate at 4°C for 1 hour. The supernatant is then removed, and 30% sucrose is added; incubate at 4°C overnight or until the organoids settle at the bottom of the tube. Remove the sucrose, stain the organoids with eosin, and carefully transfer them to a mold. Encase in optimal cutting temperature compound and incubate at 4°C for

2 to 3 hours. Freeze the block in liquid nitrogen, then either store at -80°C or section into 10 μm slices.

### 7. Immunofluorescent staining

Slides were incubated in blocking buffer (10% Donkey serum and 0.3% Triton X-100 in phosphate-buffered saline [PBS]) for 1 hour at room temperature. Sections were then incubated at 4°C overnight with primary antibodies: surfactant protein C (SFTPC; cat no. AB90716, 1:200), HTII-280 (1:500), KRT5 (cat no. AB52635, 1:500), KRT17 (cat no. sc-393002, 1:200), aquaporin 5 (AQP5; cat no. AB92320, 1:200), 4',6-diamidino-2-phenylindole (DAPI; cat no. 62248, 1:1,000). After washing with PBS, the slides were incubated with fluorophore-conjugated secondary antibodies for 1 hour at room temperature in darkness. Subsequent washes were conducted before the slides were mounted with a DAPI-containing medi-

**Figure 2.** Fluorescence-activated cell sorting (FACS) results and percentage of alveolar type 2 (AT2) cells in each group. (A) FACS results for each group, with P7 gate indicating epithelial cell adhesion molecule (EpCAM) and HT2-280 double-positive AT2 cells. (B) Percentage of EpCAM+HT2-280+ cells within total cells for each group. IPF: idiopathic pulmonary fibrosis; pnx: pneumothorax.

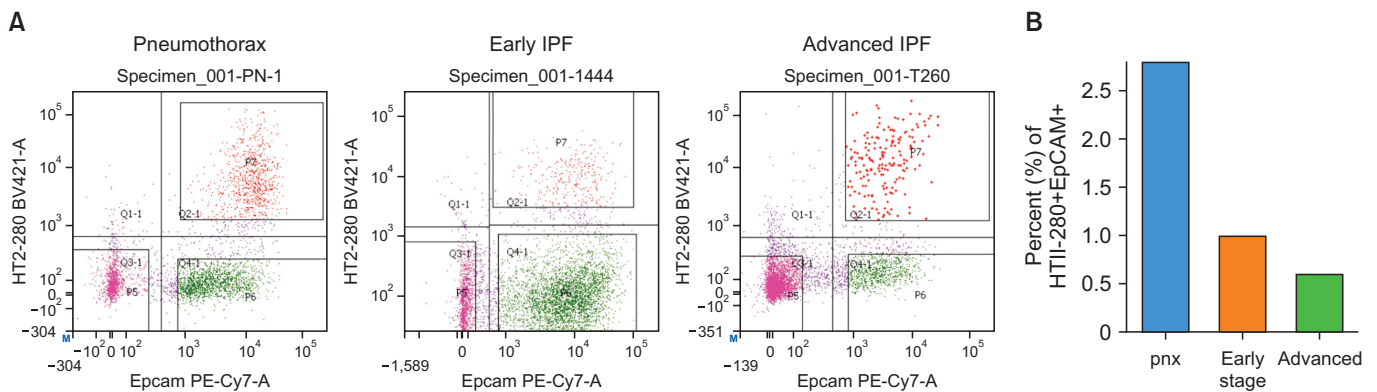
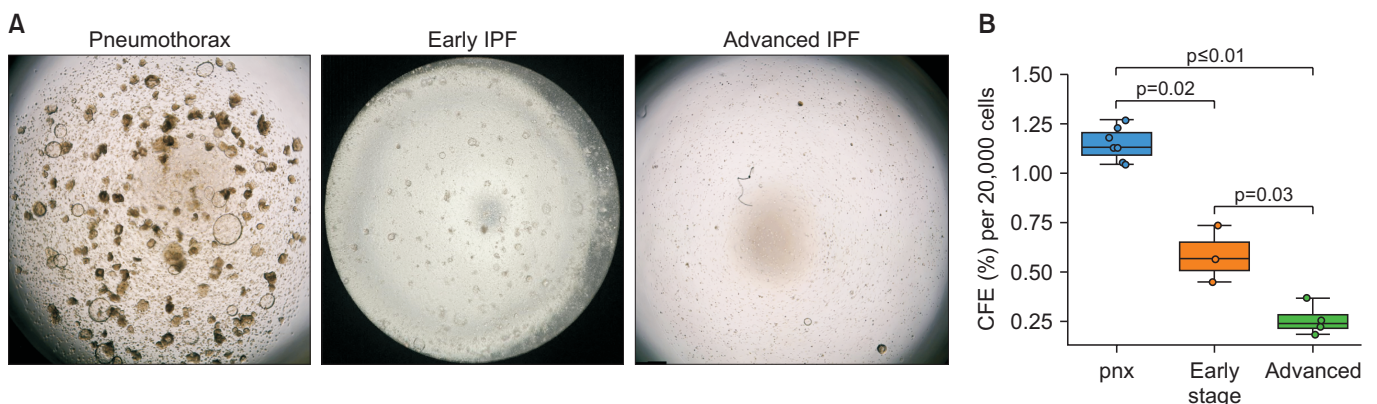


**Figure 3.** Patient derived lung organoids and colony forming efficiency (CFE) in each group. (A) Morphology of patient-derived lung organoids in each group at 3 weeks. (B) CFE (%) per 2,000 cells in each group. IPF: idiopathic pulmonary fibrosis; pnx: pneumothorax.



um to stain nuclei. Fluorescence images were acquired using a confocal microscope.

### 8. Statistical analysis

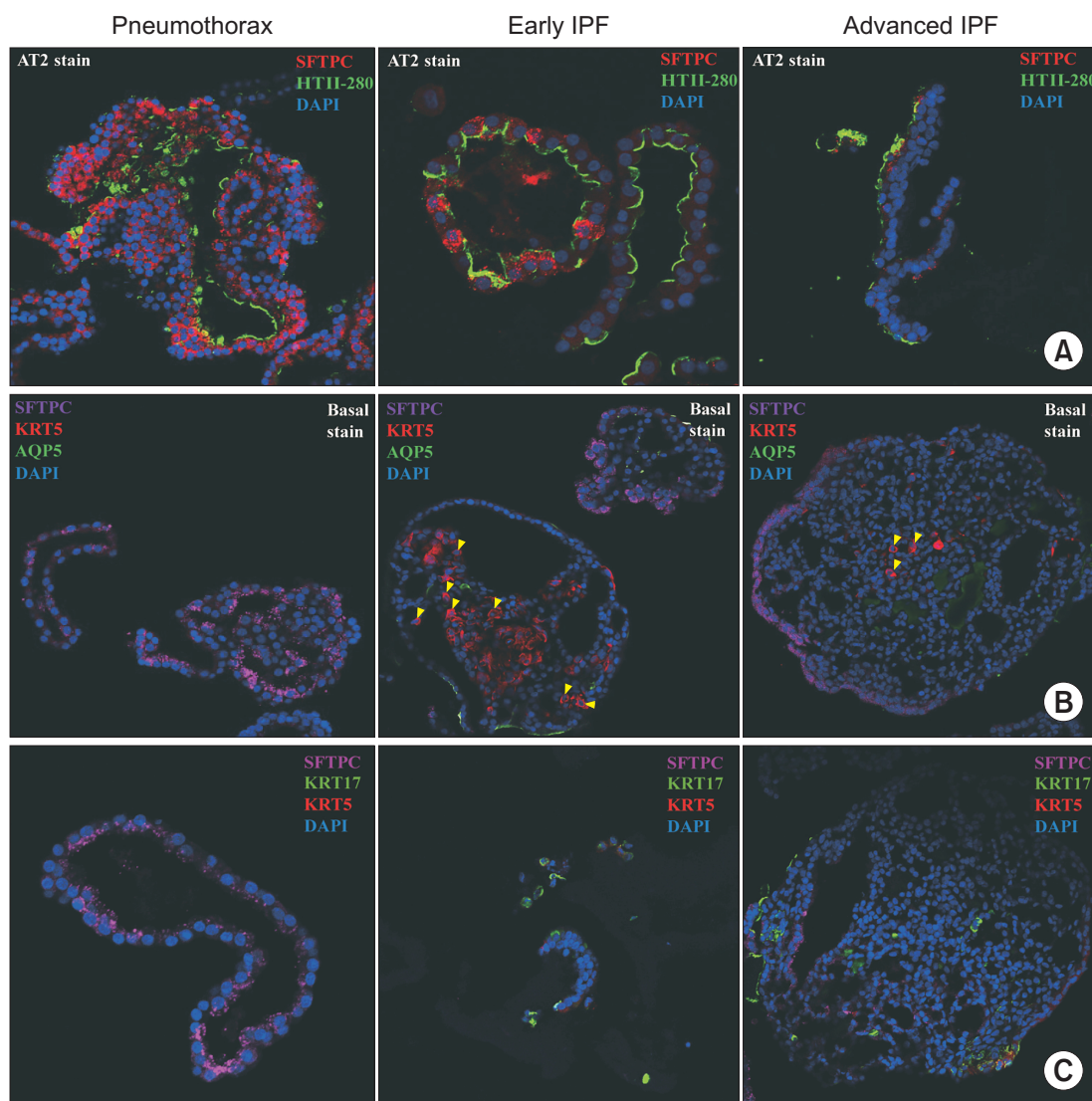
Data were analyzed using SciPy in Python. Results are presented as mean±standard deviation. Statistical significance between two groups was assessed using the Mann-Whitney U test, conducted for each pair of the three groups studied. A p-value of less than 0.05 was considered statistically significant.

## Results

### 1. Proportion of AT2 decreases following disease progression

Figure 2 demonstrates that the FACS yield of HTII-280+/EpCAM+ cells, identified as AT2, decreased as IPF progressed. Using pneumothorax tissue as the control group, we obtained 2.7% of AT2 cells from total lung cells. However, with early IPF tissue, the yield was 1.0% of AT2 cells, and with advanced IPF tissue, it was only 0.6%.

**Figure 4.** Immunostaining of lung organoids in each group. (A) Alveolar type 2 (AT2) stain (red color, surfactant protein C [SFTPC]; green color, HTII-280; blue color, 4',6-diamidino-2-phenylindole [DAPI]). (B) Basal stain (purple color, SFTPC; red color, KRT5; green color, aquaporin 5 [AQP5]; blue color, DAPI; yellow arrowheads, basal cell). (C) Basal stain (purple color, SFTPC; red color, keratin 5 [KRT5]; green color, KRT17; blue color, DAPI).



## 2. CFE in day 21 decreases following disease progression

Figure 3 reveals that on day 21, organoids cultured from sorted AT2 cells exhibited distinct characteristics in each group. Organoids derived from the pneumothorax (control) tissue formed well, as anticipated; conversely, those derived from IPF tissue were smaller and less numerous. Furthermore, organoid formation decreased progressively from the early to the advanced stages of IPF. CFE measurements showed pneumothorax organoids had a CFE of 1.1%, early IPF organoids 0.6%, and advanced IPF organoids 0.25%. Statistical analysis indicated significant differences, with p-values of 0.02 between pneumothorax and early-stage IPF, less than 0.01 between pneumothorax and advanced-stage IPF, and 0.03 between early and advanced stages of IPF.

## 3. IPF-derived organoid contains basal cells (KRT5+ cells)

Figure 4 displays the immunostaining results for cryo-sectioned organoids from each group on the 30th day. Figure 4A shows staining for the AT2 cell markers SFTPC and HTII-280, confirming the appropriate development of alveolar organoids. All groups displayed organoids with AT2 cells expressing both SFTPC and HTII-280. However, organoids derived from early and advanced stages of IPF showed weaker expression of SFTPC compared to those from the pneumothorax group. Figure 4B reveals that in the pneumothorax group, no cells tested positive for the basal cell marker KRT5, whereas in the IPF-derived organoids, KRT5+ cells were present (indicated by yellow arrowheads). Figure 4C additionally notes that, aside from KRT5, KRT17 positive cells were detected in organoids from both early and advanced stages of IPF.

## Discussion

This study aimed to create patient-derived lung organoids to compare the regenerative capacity of AT2 cells across different groups. We selected patients from three groups: control (normal lung tissue from pneumothorax patients), early-stage IPF (tissue at initial diagnosis), and advanced-stage IPF (tissue from lung transplants). The proportion of AT2 cells among the total cells was lower in the IPF groups compared to the control group. This finding aligns with the results of recently published single-cell RNA sequencing studies<sup>10,11,14</sup>. These studies also demonstrated that AT2 cells in IPF were smaller than those from transplant donors. Our study revealed that the proportion of AT2 cells declined further from early to advanced stages of

IPF, indicating that the absolute number of AT2 cells, crucial for regeneration as stem cells in the alveoli<sup>15</sup>, is reduced in IPF and continues to decrease as the disease progresses. The decrease in the proportion of AT2 cells likely contributes to the regenerative dysfunction observed in IPF<sup>16</sup>.

Next, to further explore the differences in regenerative capacity of AT2 cells, we generated patient-derived lung organoids. These organoids were created using adult stem cells and were cultured following a protocol exclusive to AT2 cells, without feeder cells<sup>13,17,18</sup>. To minimize variability associated with the number of AT2 cells seeded per well, 20,000 AT2 cells were consistently cultured in each well across all groups. On day 21, the pneumothorax-derived lung organoids showed robust growth, forming well-defined alveosphere structures. In contrast, the IPF-derived lung organoids appeared smaller and were less numerous. Furthermore, the number of organoids decreased progressively from early to advanced stages of IPF, suggesting that AT2 cells from IPF may inherently possess diminished regenerative capacity. Indeed, IPF AT2 cells have been shown to exhibit increased endoplasmic reticulum stress and apoptosis<sup>19</sup>, accompanied by senescence<sup>20,21</sup> and mitochondrial dysfunction<sup>22,23</sup>. These functional changes in AT2 cells are thought to contribute to their decreased regenerative capacity.

To confirm that the cultured organoids consisted predominantly of AT2 cells, each organoid was cryo-sectioned and immunostained. All groups contained AT2 cells expressing SFTPC and HTII-280. However, SFTPC expression was diminished in the IPF-derived organoids, with further decreases noted as the disease progressed. This indicates a surfactant production dysfunction in AT2 cells within IPF. Surfactant production dysfunction has been identified as a critical genetic mutation in both familial and sporadic IPF<sup>24,25</sup>. Moreover, studies have demonstrated that disrupting surfactant genes in mice leads to exacerbated fibrosis<sup>26</sup>. In this study, the IPF-derived organoids seem to retain the characteristic surfactant dysfunction observed in IPF AT2 cells.

Another distinctive feature observed was the presence of KRT5+ basal cells in the IPF-derived organoids, absent in the control group. Recent studies have indicated that when normal AT2 cells are co-cultured with fibroblasts from IPF patients, the AT2 cells lose their SFTPC expression and begin to express KRT8, eventually transforming into basal cells that express KRT5. This shows that normal AT2 cells can differentiate into basal cells under the influence of their surrounding niche<sup>13</sup>. This study confirmed that IPF AT2 cells can

differentiate into basal cells independently of environmental changes. It suggests that the differentiation plasticity of IPF AT2 cells is inherently altered. Several studies have highlighted that aberrant basaloid cells and basal cells play a pivotal role in IPF pathogenesis<sup>27,28</sup>. Although there is debate over the origin of basal cells<sup>29-31</sup>, the findings from this study suggest that they may arise from the altered differentiation plasticity of IPF AT2 cells.

To elucidate the differences in AT2 cell characteristics in IPF organoids, single-cell RNA sequencing of IPF-derived organoids is proposed. This method will more precisely identify the cell types within the organoids compared to immunostaining, revealing which cells can evolve from AT2 cells. If specific gene variations are detected, siRNA or Clustered Regularly Interspaced Short Palindromic Repeats (CRISPR) can be employed to inhibit these genes to assess whether changes in AT2 cell characteristics can be obstructed.

Our study has three limitations. First, the purity of AT2 cells sorted by MACS is not perfect, leading to potential contamination by other cells in the cultured AT2 cells. To reduce contamination and increase purity, FACS can be used. However, as IPF progresses, the availability of AT2 cells diminishes, necessitating a larger tissue sample. Second, we used the HTII-280 antibody to sort AT2 cells, but it remains unconfirmed how specifically HTII-280 binds to AT2 cells in IPF lungs compared to normal lung tissue, although it is commonly used as a marker for AT2 cells. This specificity could be further confirmed by comparing the cells sorted with HTII-280 through RNA sequencing with normal AT2 cells. Third, our pneumothorax samples (normal) were from younger individuals compared to the IPF samples, and all were non-smokers. It may be challenging to exclude the effects of age and smoking history on AT2 cells in this study. Further validation with normal samples of similar age and smoking history is likely necessary. Additionally, the sample size was small, necessitating confirmation by studies with larger sample sizes.

In conclusion, this study confirmed that the regenerative capacity of AT2 cells in IPF decreases as the disease advances. It also found that IPF AT2 cells inherently exhibit functional anomalies, such as impaired surfactant production and altered differentiation plasticity.

## Authors' Contributions

Conceptualization: Park MS. Methodology: Choi J, Lee JH, Kim CH. Formal analysis: Choi HK. Data curation: Shin JH, Shin MH, Shim HS, Suh YJ. Funding acquisi-

tion: Kim CH, Park MS. Project administration: Woo A, Kim SY, Lee SH, Kim EY. Visualization: Choi HK. Software: Choi HK. Validation: Choi HK. Investigation: Choi HK, Bang G, Kim HE, Lee JG. Writing - original draft preparation: Choi HK. Writing - review and editing: Choi HK. Approval of final manuscript: all authors.

## Conflicts of Interest

No potential conflict of interest relevant to this article was reported.

## Funding

This research was supported by a grant of the MD-Phd/Medical Scientist Training Program through the Korea Health Industry Development Institute (KHIDI), funded by the Ministry of Health & Welfare, Republic of Korea.

## References

1. Martinez FJ, Collard HR, Pardo A, Raghu G, Richeldi L, Selman M, et al. Idiopathic pulmonary fibrosis. *Nat Rev Dis Primers* 2017;3:17074.
2. Koudstaal T, Wijsenbeek MS. Idiopathic pulmonary fibrosis. *Presse Med* 2023;52:104166.
3. Lee SH, Yeo Y, Kim TH, Lee HL, Lee JH, Park YB, et al. Korean guidelines for diagnosis and management of interstitial lung diseases: part 2. idiopathic pulmonary fibrosis. *Tuberc Respir Dis (Seoul)* 2019;82:102-17.
4. Idiopathic Pulmonary Fibrosis Clinical Research Network; Raghu G, Anstrom KJ, King TE Jr, Lasky JA, Martinez FJ. Prednisone, azathioprine, and N-acetylcysteine for pulmonary fibrosis. *N Engl J Med* 2012;366:1968-77.
5. Mei Q, Liu Z, Zuo H, Yang Z, Qu J. Idiopathic pulmonary fibrosis: an update on pathogenesis. *Front Pharmacol* 2022;12:797292.
6. Zhang K, Xu L, Cong YS. Telomere dysfunction in idiopathic pulmonary fibrosis. *Front Med (Lausanne)* 2021;8:739810.
7. Alder JK, Chen JJ, Lancaster L, Danoff S, Su SC, Cogan JD, et al. Short telomeres are a risk factor for idiopathic pulmonary fibrosis. *Proc Natl Acad Sci U S A* 2008;105:13051-6.
8. Naikawadi RP, Disayabutr S, Mallavia B, Donne ML, Green G, La JL, et al. Telomere dysfunction in alveolar epithelial cells causes lung remodeling and fibrosis. *JCI Insight* 2016;1:e86704.
9. Pineiro-Hermida S, Martinez P, Bosso G, Flores JM, Saraswati S, Connor J, et al. Consequences of telomere dysfunction in fibroblasts, club and basal cells for lung

- fibrosis development. *Nat Commun* 2022;13:5656.
10. Adams TS, Schupp JC, Poli S, Ayaub EA, Neumark N, Ahangari F, et al. Single-cell RNA-seq reveals ectopic and aberrant lung-resident cell populations in idiopathic pulmonary fibrosis. *Sci Adv* 2020;6:eaba1983.
  11. Habermann AC, Gutierrez AJ, Bui LT, Yahn SL, Winters NI, Calvi CL, et al. Single-cell RNA sequencing reveals profibrotic roles of distinct epithelial and mesenchymal lineages in pulmonary fibrosis. *Sci Adv* 2020;6:eaba1972.
  12. Moss BJ, Ryter SW, Rosas IO. Pathogenic mechanisms underlying idiopathic pulmonary fibrosis. *Annu Rev Pathol* 2022;17:515-46.
  13. Kathiriya JJ, Wang C, Zhou M, Brumwell A, Cassandras M, Le Saux CJ, et al. Human alveolar type 2 epithelium trans-differentiates into metaplastic KRT5+ basal cells. *Nat Cell Biol* 2022;24:10-23.
  14. Xu Y, Mizuno T, Sridharan A, Du Y, Guo M, Tang J, et al. Single-cell RNA sequencing identifies diverse roles of epithelial cells in idiopathic pulmonary fibrosis. *JCI Insight* 2016;1:e90558.
  15. Barkauskas CE, Cronce MJ, Rackley CR, Bowie EJ, Keene DR, Stripp BR, et al. Type 2 alveolar cells are stem cells in adult lung. *J Clin Invest* 2013;123:3025-36.
  16. Wang ZN, Tang XX. New perspectives on the aberrant alveolar repair of idiopathic pulmonary fibrosis. *Front Cell Dev Biol* 2020;8:580026.
  17. Youk J, Kim T, Evans KV, Jeong YI, Hur Y, Hong SP, et al. Three-dimensional human alveolar stem cell culture models reveal infection response to SARS-CoV-2. *Cell Stem Cell* 2020;27:905-19.
  18. Choi J, Jang YJ, Dabrowska C, Ilich E, Evans KV, Hall H, et al. Release of Notch activity coordinated by IL-1 $\beta$  signaling confers differentiation plasticity of airway progenitors via *Fosl2* during alveolar regeneration. *Nat Cell Biol* 2021;23:953-66.
  19. Korfei M, Ruppert C, Mahavadi P, Henneke I, Markart P, Koch M, et al. Epithelial endoplasmic reticulum stress and apoptosis in sporadic idiopathic pulmonary fibrosis. *Am J Respir Crit Care Med* 2008;178:838-46.
  20. Yamada Z, Nishio J, Motomura K, Mizutani S, Yamada S, Mikami T, et al. Senescence of alveolar epithelial cells impacts initiation and chronic phases of murine fibrosing interstitial lung disease. *Front Immunol* 2022;13:935114.
  21. Tu M, Wei T, Jia Y, Wang Y, Wu J. Molecular mechanisms of alveolar epithelial cell senescence and idiopathic pulmonary fibrosis: a narrative review. *J Thorac Dis* 2023;15:186-203.
  22. Chung KP, Hsu CL, Fan LC, Huang Z, Bhatia D, Chen YJ, et al. Mitofusins regulate lipid metabolism to mediate the development of lung fibrosis. *Nat Commun* 2019;10:3390.
  23. Cloonan SM, Kim K, Esteves P, Triani T, Barnes PJ. Mitochondrial dysfunction in lung ageing and disease. *Eur Respir Rev* 2020;29:200165.
  24. Wasnick R, Korfei M, Piskulak K, Henneke I, Wilhelm J, Mahavadi P, et al. Notch1 induces defective epithelial surfactant processing and pulmonary fibrosis. *Am J Respir Crit Care Med* 2023;207:283-99.
  25. Sutton RM, Bittar HT, Sullivan DI, Silva AG, Bahudhanapati H, Parikh AH, et al. Rare surfactant-related variants in familial and sporadic pulmonary fibrosis. *Hum Mutat* 2022;43:2091-101.
  26. Lawson WE, Polosukhin VV, Stathopoulos GT, Zoia O, Han W, Lane KB, et al. Increased and prolonged pulmonary fibrosis in surfactant protein C-deficient mice following intratracheal bleomycin. *Am J Pathol* 2005;167:1267-77.
  27. Jaeger B, Schupp JC, Plappert L, Terwolbeck O, Artysh N, Kayser G, et al. Airway basal cells show a dedifferentiated KRT17<sup>high</sup> phenotype and promote fibrosis in idiopathic pulmonary fibrosis. *Nat Commun* 2022;13:5637.
  28. Hewitt RJ, Puttur F, Gaboriau DC, Fercoq F, Fresquet M, Traves WJ, et al. Lung extracellular matrix modulates KRT5+ basal cell activity in pulmonary fibrosis. *Nat Commun* 2023;14:6039.
  29. Li X, An G, Wang Y, Liang D, Zhu Z, Tian L. Targeted migration of bone marrow mesenchymal stem cells inhibits silica-induced pulmonary fibrosis in rats. *Stem Cell Res Ther* 2018;9:335.
  30. Zhao FY, Cheng TY, Yang L, Huang YH, Li C, Han JZ, et al. G-CSF inhibits pulmonary fibrosis by promoting BMSC homing to the lungs via SDF-1/CXCR4 chemotaxis. *Sci Rep* 2020;10:10515.
  31. Zhao X, Wu J, Yuan R, Li Y, Yang Q, Wu B, et al. Adipose-derived mesenchymal stem cell therapy for reverse bleomycin-induced experimental pulmonary fibrosis. *Sci Rep* 2023;13:13183.